Amphiphilic Scorpion-like Macromolecules: Design, Synthesis, and Characterization

Lu Tian, Larry Yam, Nan Zhou, Henry Tat, and Kathryn E. Uhrich*

Department of Chemistry and Chemical Biology, Rutgers University, 610 Taylor Road, Piscataway, New Jersey 08854

Received August 4, 2003; Revised Manuscript Received November 4, 2003

ABSTRACT: A series of novel amphiphilic scorpion-like macromolecules (AScMs) were designed for optimized drug encapsulation and transport. The branched hydrophobic domains were prepared by acylation of mucic acid with varying chain lengths of acyl chlorides. Monohydroxylated poly(ethylene glycol) (PEG) was conjugated onto the hydrophobic domain to form the final polymers. Fluorescence spectroscopy and dynamic light scattering were performed to determine the critical micelle concentrations (cmc) and aggregation particle sizes, respectively. By changing the length of PEG and acyl chains, the physicochemical properties (e.g., M_w, HLB, T_m, cmc) of AScMs are controlled. Low cmc values (10^{-5}−10^{-7} mol/L) and small particle sizes (10−20 nm) of AScMs are potentially applicable for lipophilic drug delivery applications.

Introduction

Amphiphilic macromolecules can form micellar structures in aqueous solution that are capable of carrying hydrophobic drugs,[1−16] similar to naturally occurring molecular carriers such as lipoproteins.[17] Polymeric micelles encapsulate the lipophilic drug molecules within the hydrophobic core, thus solubilizing the drug in solution with the hydrophilic shell. In addition to compartmentalization of hydrophobic drugs, the amphiphilic macromolecules must meet further criteria to be effective drug carriers. Biocompatibility, appropriate size (10−100 nm) for blood circulation, and a low critical micelle concentration (cmc) are important characteristics that lead to improved bioavailability, reduction of toxicity, enhanced permeability across physiological barriers, and substantial changes in drug biodistribution.[18−23] However, few amphiphilic macromolecules for drug delivery have been systematically evaluated, whereby the polymer composition (e.g., hydrophobic core block length) is varied and the resultant effect on the micellar properties including size, stability, loading capacity, and release kinetics is measured. With a comprehensive understanding of their chemical compositions and corresponding relationship to physical properties, amphiphilic macromolecules can be designed for optimal drug delivery.

In this paper, a series of novel amphiphilic macromolecules referred to as amphiphilic scorpion-like macromolecules (AScM; **1** in Scheme 1) were developed for colloidal drug delivery. To optimize the polymers for drug delivery, our design criteria for the amphiphilic macromolecules are fourfold. First, a tunable hydrophilic−lipophilic balance (HLB) is desired to match the amphiphilic drug carriers with the specific hydrophobicity of a drug, thus optimizing the drug−carrier interactions. Second, the drug delivery systems themselves should not cause any undesirable biological complications, such as toxicity and immunogenicity.[24] Third, the polymers should be biodegradable and easily excreted from living systems. Last, the inclusion of biological functionality, such as a targeting moiety, will significantly aid in the selective drug transport and delivery.

We prepared a series of AScMs that meet these four criteria. The macromolecules are synthesized from mucic acid (**2**), monohydroxypoly(ethylene glycol) (PEG), and acyl chlorides (**3**) (Scheme 1). These AScMs systems are referred to as M_xP_y, in which M denotes mucic acid, x denotes the total carbon number of each acyl chain, P denotes PEG, and y refers to molecular weight of the PEG in thousands. Mucic acid (**2**) has four hydroxyl groups that are acylated by a series of acyl chlorides (**3**) with varying chain lengths. The alkyl chain lengths are tuned to tailor the structure and properties of the resulting polymers. The multibranched hydrophobic domain of **4** is proposed to be more efficient in self-assembly in aqueous media than a single hydrophobic block.[25,26] Mucic acid (**2**) also has two carboxylic acid groups, which can be selectively activated and conjugated to bioactive molecules. Finally, mucic acid (**2**) is a naturally occurring compound,[27,28] which enhances the biocompatibility of the final polymers.[29]

PEG was chosen for its well-known biological significance.[30−32] An important aspect of PEG is its tremendous water solubility and hydrophilicity; a significant amount of water molecules can be bound onto polymer backbone via H-bonds.[33] The high flexibility and large exclusion volume of PEG[34,35] in water provide another advantage of PEG over other hydrophilic polymers. With a PEG-based shell, microparticles such as micelles and liposomes as well as nanoparticles can avoid the adsorption of proteins and adhesion of cells in biological media.[10]

Similar to conventional amphiphilic diblock copolymers,[30−32] the M_xP_y systems have a hydrophilic block (i.e., PEG) that is modified by a hydrophobic portion (i.e., acylated mucic acid derivatives, **4**). Unlike amphiphilic diblock copolymers, the hydrophobic component of the M_xP_y materials is multibranched. We propose that the extremely hydrophobic, multibranched domain will contribute to forming a stable aggregation in an aqueous system, which is ultimately a function of HLB. Herein, we report the synthesis and physicochemical characterization of the M_xP_y systems, including their micellar behavior.

* To whom correspondence should be addressed: phone (732) 445 0361; Fax (732) 445 7036; e-mail Uhrich@rutchem.rutgers.edu.

10.1021/ma030411a CCC: $27.50
Published on Web 12/18/2003

Scheme 1

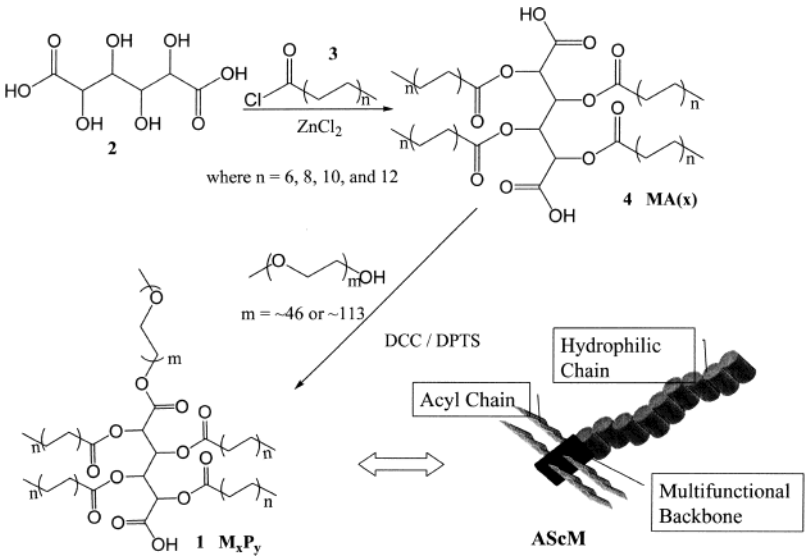

Experimental Section

Materials. TLC plates (Whatman, AL SIL G/UV), ethyl ether, ethanol, and petroleum ether were purchased from Fisher and used as received. Bromophenol indicator was prepared by 0.5% of bromophenol blue (Bio-Rad Laboratories, Hercules, CA) in ethanol, made slightly alkaline (pH ~ 12) with NaOH (pellets). 4-(Dimethylamino)pyridinium *p*-toluenesulfonate (DPTS) was prepared as described by Moore and Stupp.[36] Methylene chloride was distilled over calcium hydride. All other chemicals were obtained from Aldrich and used as received.

Methods. ^{1}H NMR spectra were recorded on Varian 200 and 400 MHz spectrometers. Samples (~5−10 mg/mL) were dissolved in $CDCl_3$ or d_8-THF, with TMS as an internal reference. IR spectra were recorded on a Mattson series spectrophotometer by solvent-casting samples onto a KBr pellet. Mass spectrometry was done on ThermoQuest Finnigan LCQ_{DUO} system that includes a syringe pump, an optional divert/inject valve, an atmospheric pressure ionization (API) source, a mass spectrometer (MS) detector, and the Xcalibur data system.

A Thomas-Hoover capillary melting apparatus was used to determine the melting points of mucic acid derivatives (**4**). The heating rate was maintained at 5 °C/min; each sample's melting point was measured three times with deviations within 2.0 °C. The melting point was reported as the range between the averaged lower end and averaged higher end temperatures.

Gel permeation chromatography was performed on a Perkin-Elmer series 200 LC system equipped with a PL-Gel column (5 μm, mixed bed, i.d. 7.8 mm, length 300 mm) operated at 60 °C, a series 200 refractive index detector, a series 200 LC pump, and an ISS 200 autosampler. A digital Celebris 466 computer was used to automate the analysis via PE Nelson 900 interface and PE Nelson 600 Link box. Perkin-Elmer Turbochrom 4 software was used for data collection as well as data processing. Tetrahydrofuran (THF) was used as eluent for analysis and solvent for sample preparation. The sample (~5 mg/mL) was dissolved into THF and filtered using a 0.45 μm PTFE syringe filter (Whatman, Clifton, NJ) before injection into the column at a flow rate of 0.5 mL/min. The average molecular weight of the sample was calibrated against narrow molecular weight polystyrene standards (Polysciences, Warrington, PA).

Thermal analysis was performed on a Perkin-Elmer system consisting of a Pyris 1 DSC analyzer with TAC 7/DX instrument controllers. PE Pyris software was used for data collection and processing on a DEC Venturis 5100 computer. For differential scanning calorimetry (DSC), samples (~10 mg) were heated under dry nitrogen gas. Data were collected at heating and cooling rates of 10 °C/min with a three-cycle minimum.

Intrinsic viscosities of the polymer solutions were determined using an Ubbelohde viscometer (Cannon, size 150) according to ASTM D445 and ISO 3104 at 25 °C. Each sample was measured in triplicate. The intrinsic viscosity values were obtained by multiplying the efflux time by the viscometer constant (0.033 59 mm^2/s^2, as determined by the manufacturer). Above concentrations of 10^{-3} mol/L, the intrinsic viscosity of each M_xP_y solution linearly decreased upon dilution. At concentrations below 10^{-3} M, the intrinsic viscosity of all solutions remained constant.

Fluorescence studies[37−39] were carried out on a Spex fluoroMax spectrofluorometer (Piscataway, NJ) at 25 °C. Using pyrene as the probe molecule, a stock solution at 5.00×10^{-7} M in water was prepared. Polymer samples were dissolved in the stock pyrene solution, then diluted to specific concentrations. Excitation was performed from 300 to 360 nm, with 390 nm as the emission wavelength. With micelle formation, the pyrene maximum absorption shifted from 332 to 334.5 nm. The ratio of absorption of pyrene with polymer (334.5 nm) to pyrene only (332 nm) was plotted as the logarithm of polymer concentrations. The inflection point of the curve was taken as the cmc.[38,39]

Dynamic light scattering analyses were performed on aqueous solutions by photon correlation spectroscopy using a PSS Nicomp 380 submicron particle sizer instrument (Particle Sizing Systems, Inc., Santa Barbara, CA). A 20 mW, 523 nm diode-pumped solid-state laser module and an avalanche photodiode detector were used. Measurements were performed at a 90° scattering angle at 25 °C. The viscosities were set to the values determined by viscosity measurements as described above, and the index of refraction was set to that of the sample vials (1.33). The data were analyzed using Nicomp number-weighted analysis and multimodal Laplace transform analysis.

Preparation of Mucic Acid Derivatives (4). The preparation of MA(12) is presented as an example.

MA(12). Mucic acid (**2**) (4.2 g, 20 mmol) and zinc chloride (0.28 g, 2.0 mmol) were added into lauroyl chloride (37 mL, 160 mmol). The reaction mixture was heated to 90 °C for 10−12 h. After cooling to room temperature, diethyl ether (20 mL) was added to the reaction mixture, and the solution was poured into ice water (~150 mL) with stirring. Additional diethyl ether (80 mL) was added to the mixture and stirring continued for another 30 min. The ether portion was separated, washed with brine to neutral pH (~7), dried over anhydrous sodium sulfate, and evaporated to dryness. The crude product was purified by precipitation into petroleum ether (200 mL) from diethyl ether (20 mL). Product was obtained as white

powder (13 g, 68% yield). FW: 939.4; MS: 938.7. ^{1}H NMR (d_8-THF) (δ): 5.71 (s, 2H, C*H*), 5.12 (s, 2H, C*H*), 2.40 (t, 4H, CH_2), 2.28 (t, 4H, CH_2), 1.63 (m, 4H, CH_2), 1.57 (m, 4H, CH_2), 1.29 (m, 64H, CH_2), 0.92 (t, 12H, CH_3). IR (KBr, cm^{-1}): 1750, 1728 (C=O), 1245, 1169 (C−O). T_m = 156−157 °C.

MA(10). Product was obtained as white powder (13 g, 79% yield). FW: 827.1; MS: 826.6. ^{1}H NMR ($CDCl_3$) (δ): 5.74 (s, 2H, C*H*), 5.20 (s, 2H, C*H*), 2.47 (t, 4H, CH_2), 2.32 (t, 4H, CH_2), 1.66 (m, 4H, CH_2), 1.58 (m, 4H, CH_2), 1.35 (m, 48H, CH_2), 0.93 (t, 12H, CH_3). IR (KBr, cm^{-1}): 1754, 1732 (C=O), 1252, 1166 (C−O). T_m = 159−160 °C.

MA(8). Product was obtained as white powder (10 g, 70% yield). FW: 714.9; MS: 714.5. ^{1}H NMR ($CDCl_3$) (δ): 5.71 (s, 2H, C*H*), 5.18 (s, 2H, C*H*), 2.44 (t, 4H, CH_2), 2.31 (t, 4H, CH_2), 1.64 (m, 4H, CH_2), 1.55 (m, 4H, CH_2), 1.28 (m, 32H, CH_2), 0.86 (t, 12H, CH_3). IR (KBr, cm^{-1}): 1755, 1731 (C=O), 1249, 1167 (C−O). T_m = 165−166 °C.

MA(6). Product was obtained as white powder (10 g, 84% yield). FW: 602.72; MS: 602.3. ^{1}H NMR ($CDCl_3$) (δ): 5.71 (s, 2H, C*H*), 5.18 (s, 2H, C*H*), 2.45 (t, 4H, CH_2), 2.31 (t, 4H, CH_2), 1.63 (m, 4H, CH_2), 1.55 (m, 4H, CH_2), 1.30 (m, 16H, CH_2), 0.91 (t, 12H, CH_3). IR (KBr, cm^{-1}): 1751, 1734 (C=O), 1243, 1162 (C−O). T_m = 170−171 °C.

Preparation of AScMs (1). The preparation of $M_{12}P_5$ is presented as an example.

$M_{12}P_5$. PEG (M_w = 5.0 kDa) (5.0 g, 1.0 mmol) was dehydrated by azeotropic distillation in toluene (30 mL) for 1 h, and toluene was removed under vacuum. MA(12) (2.8 g, 3.0 mmol) and DPTS (0.31 g, 1.0 mmol) in methylene chloride (30 mL) were added at room temperature. DMF (3.0 mL) was also added to ensure a clear, homogeneous solution. After 10 min under nitrogen, 4.0 mL of DCC solution (1.0 M in methylene chloride) was added dropwise over 15 min. After 24 h, the DCC side product (dicyclohexylurea) was removed by suction filtration. The filtrate was washed with 20 mL portions of brine (5×), dried over anhydrous sodium sulfate, and evaporated to dryness. The crude product was purified by precipitation into diethyl ether (100 mL) from methanol (5 mL). Product was obtained as a white, waxy solid (5.8 g, 98% yield). The ethylene oxide of PEG comprises a significant component of AScM and dominates the ^{1}H NMR and IR spectra. ^{1}H NMR ($CDCl_3$) (δ): 5.70 (m, 2H, C*H*), 5.16 (m, 2H, C*H*), 3.63 (m, ∼0.4kH, CH_2), 2.41 (t, 4H, CH_2), 2.26 (t, 4H, CH_2), 1.64 (m, 4H, CH_2), 1.53 (m, 4H, CH_2), 1.26 (m, 64H, CH_2), 0.88 (t, 12H, CH_3). IR (KBr, cm^{-1}): 2891 (C−H), 1753 (C=O), 1242, 1149, 1114 (C−O). T_m = 56.4 °C (peak value by DSC); GPC: M_w = 5.9 kDa; PDI = 1.06.

$M_{10}P_5$. Product was obtained as a white, waxy solid (5.5 g, 94% yield). ^{1}H NMR ($CDCl_3$) (δ): 5.69 (m, 2H, C*H*), 5.17 (m, 2H, C*H*), 3.66 (m, ∼0.4kH, CH_2), 2.42 (t, 4H, CH_2), 2.28 (t, 4H, CH_2), 1.62 (m, 4H, CH_2), 1.53 (m, 4H, CH_2), 1.28 (m, 48H, CH_2), 0.88 (t, 12H, CH_3). IR (KBr, cm^{-1}): 2925, 2890 (C−H), 1752 (C=O), 1250, 1148, 1112 (C−O). T_m = 57.8 °C (peak value by DSC); GPC: M_w = 5.5 kDa; PDI = 1.08.

M_8P_5. Product was obtained as a white, waxy solid (5.6 g, 98% yield). ^{1}H NMR ($CDCl_3$) (δ): 5.70 (m, 2H, C*H*), 5.18 (m, 2H, C*H*), 3.63 (m, ∼0.4kH, CH_2), 2.43 (t, 4H, CH_2), 2.29 (t, 4H, CH_2), 1.64 (m, 4H, CH_2), 1.55 (m, 4H, CH_2), 1.29 (m, 32H, CH_2), 0.88 (t, 12H, CH_3). IR (KBr, cm^{-1}): 2892 (C−H), 1752 (C=O), 1243, 1152, 1114 (C−O). T_m = 57.1 °C (peak value by DSC); GPC: M_w = 5.4 kDa; PDI = 1.07.

M_6P_5. Product was obtained as a white, waxy solid (5.2 g, 93% yield). ^{1}H NMR ($CDCl_3$) (δ): 5.68 (m, 2H, C*H*), 5.17 (m, 2H, C*H*), 3.65 (m, ∼0.4kH, CH_2), 2.43 (t, 4H, CH_2), 2.30 (t, 4H, CH_2), 1.62 (m, 4H, CH_2), 1.53 (m, 4H, CH_2), 1.32 (m, 16H, CH_2), 0.88 (t, 12H, CH_3). IR (KBr, cm^{-1}): 2891 (C−H), 1752 (C=O), 1250, 1142, 1113 (C−O). T_m = 59.3 °C (peak value by DSC); GPC: M_w = 5.3 kDa, PDI = 1.08.

$M_{12}P_2$. Product was obtained as white waxy solid (2.8 g, 95% yield). ^{1}H NMR ($CDCl_3$) (δ): 5.72 (m, 2H, C*H*), 5.19 (m, 2H, C*H*), 3.64 (m, ∼0.2kH, CH_2), 2.43 (t, 4H, CH_2), 2.30 (t, 4H, CH_2), 1.68 (m, 4H, CH_2), 1.54 (m, 4H, CH_2), 1.25 (m, 64H, CH_2), 0.88 (t, 12H, CH_3). IR (KBr, cm^{-1}): 2926, 2873 (C−H), 1752 (C=O), 1245, 1143, 1106 (C−O). T_m = 45.4 °C (peak value by DSC); GPC: M_w = 2.8 kDa, PDI = 1.09.

$M_{10}P_2$. Product was obtained as a white, waxy solid (2.7 g, 96% yield). ^{1}H NMR ($CDCl_3$) (δ): 5.71 (m, 2H, C*H*), 5.20 (m, 2H, C*H*), 3.70 (m, ∼0.2kH, CH_2), 2.43 (t, 4H, CH_2), 2.29 (t, 4H, CH_2), 1.67 (m, 4H, CH_2), 1.54 (m, 4H, CH_2), 1.29 (m, 48H, CH_2), 0.89 (t, 12H, CH_3). IR (KBr, cm^{-1}): 2925, 2891 (C−H), 1757 (C=O), 1243, 1147, 1111 (C−O). T_m = 45.2 °C (peak value by DSC); GPC: M_w = 2.6 kDa, PDI = 1.11.

M_8P_2. Product was obtained as a white, waxy solid (2.5 g, 92% yield). ^{1}H NMR ($CDCl_3$) (δ): 5.68 (m, 2H, C*H*), 5.17 (m, 2H, C*H*), 3.69 (m, ∼0.2kH, CH_2), 2.44 (t, 4H, CH_2), 2.29 (t, 4H, CH_2), 1.63 (m, 4H, CH_2), 1.53 (m, 4H, CH_2), 1.26 (m, 32H, CH_2), 0.88 (t, 12H, CH_3). IR (KBr, cm^{-1}): 2917, 2886 (C−H), 1752 (C=O), 1252, 1145, 1106 (C−O). T_m = 46.9 °C (peak value by DSC); GPC: M_w = 2.5 kDa, PDI = 1.05.

M_6P_2. Product was obtained as a white, waxy solid (2.5 g, 97% yield). ^{1}H NMR ($CDCl_3$) (δ): 5.70 (m, 2H, C*H*), 5.17 (m, 2H, C*H*), 3.65 (m, ∼0.2kH, CH_2), 2.43 (t, 4H, CH_2), 2.30 (t, 4H, CH_2), 1.64 (m, 4H, CH_2), 1.56 (m, 4H, CH_2), 1.32 (m, 16H, CH_2), 0.87 (t, 12H, CH_3). IR (KBr, cm^{-1}): 2885 (C−H), 1752 (C=O), 1243, 1149, 1114 (C−O). T_m = 45.5 °C (peak value by DSC); GPC: M_w = 2.4 kDa, PDI = 1.05.

Results and Discussion

Synthesis of Amphiphilic Macromolecules. In brief, the hydroxyl groups of mucic acid (**2**) were acylated using acyl chlorides (**3**) with varying chain lengths, where the total carbon numbers of acyl chains were 6, 8, 10, and 12. Zinc chloride was added as catalyst, and the reactions were performed using acyl chloride as solvent at 90 °C. The acylated derivatives (**4**) of mucic acid (**2**) are referred to as MA(*x*), in which *x* stands for total carbon numbers of each acyl chain. The coupling of MA(*x*) (**4**) onto the monohydroxyl-substituted PEG was accomplished with 1,3-dicyclohexylcarbodiimide (DCC) as coupling agent and DPTS as catalyst[36] to yield the amphiphilic polymers (M_xP_y), **1** (Scheme 1).

Mucic acid (**2**) is a water-soluble sugar that is not soluble in most common organic solvents; thus, the acylation of mucic acid was performed in neat acyl chloride. The completion of acylation was monitored by NMR spectroscopy, specifically by observing the methine proton resonance shift from 4−5 to 5−6 ppm. Upon completion of the reaction, the excess acyl chloride as well as unwanted anhydride bonds between various carboxylic acids was hydrolyzed in the aqueous workup. The colored impurities of the crude reaction products were removed upon precipitation. All the acylation products (**4**) were pure as determined by MS.

After evaluating several dehydrating agents and methods, DCC with DPTS was identified as the most appropriate coupling agent for the preparation of the final polymers M_xP_y (**1**). The crude reaction mixture was monitored by GPC for the formation of the final product (**1**). Upon the completion, a clear shift from the characteristic peak of m-PEG-OH to the product was noted in the GPC trace with no polydispersity changes. For example, the retention time of $M_{12}P_2$ (PDI = 1.10) is 16.1 min, relative to 17.0 min for the m-PEG-OH 2K (PDI = 1.11) (Figure 2). To optimize the coupling efficacy, it was critical to dry all starting materials (50 °C, 0.8 mmHg, 12 h). Additionally, m-PEG-OH was dehydrated by azeotropic distillation in toluene to remove the water associated with the PEG chains via hydrogen bonding.[40,41]

Thermal Stability. By studying the thermal stability of bulk polymer materials, one can evaluate the relationship between chemical structure and fundamental physical properties, which may correlate to in-vivo stability of the materials. The melting point (T_m) profiles

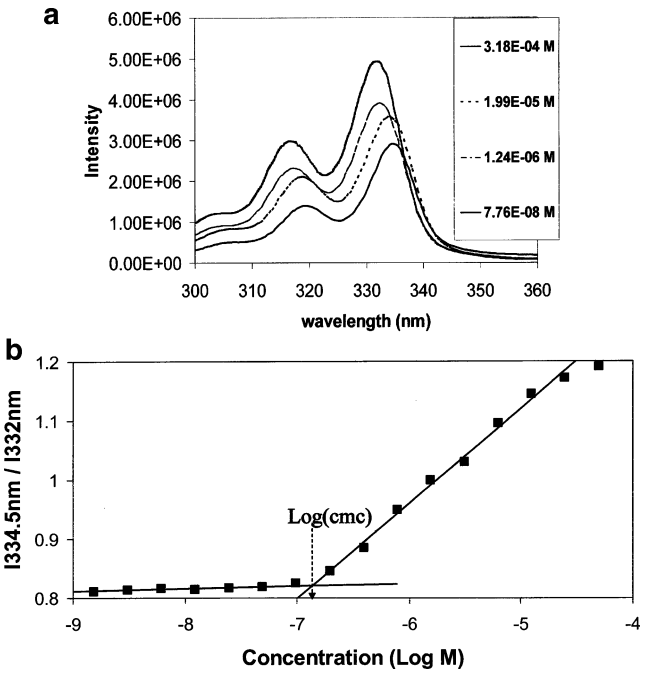

Figure 1. (a) Pyrene fluorescence excitation spectra of $M_{12}P_5$ aqueous solutions ($\lambda_{emission} = 390$ nm). (b) Fluorescence intensity ratios of pyrene excitation bands ($I_{334.5nm}/I_{332nm}$) as a function of the concentration of $M_{12}P_5$ aqueous solutions.

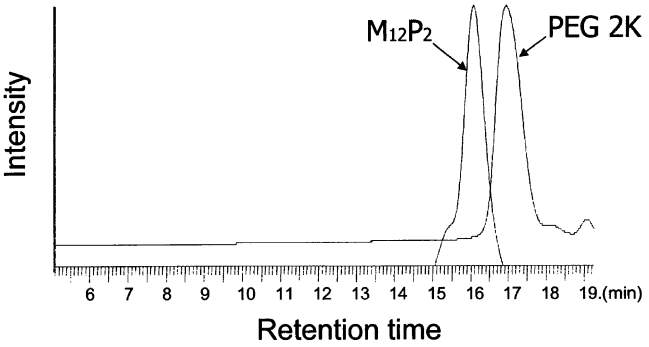

Figure 2. GPC chromatograms illustrating the differences in retention times between $M_{12}P_2$ and PEG ($M_w = 2000$).

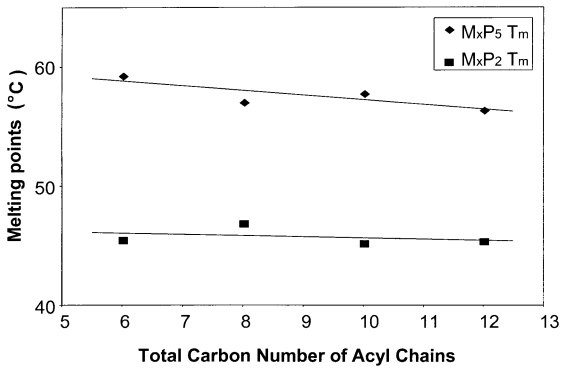

Figure 3. Relationship between the alkyl chain length and polymer melting points for each M_xP_y series. Reference compounds and their corresponding melting temperatures are PEG 5K at 63.0 °C, PEG 2K at 56.8 °C, MA(6) at 170 °C, MA(8) at 165 °C, MA(10) at 159 °C, and MA(12) at 156 °C.

of the M_xP_y series (Figure 3) were measured to determine how the hydrophobic domain size affects the thermal properties of the final polymers. The data are clustered, according to the molecular weights (2000 and 5000) of the poly(ethylene glycol) used. Relative to PEG 5K (T_m: 63.0 °C), the melting temperatures for the M_xP_5 series decreased by 4−7 °C upon increasing the length of acyl chains. Relative to PEG 2K (T_m: 56.8 °C), the melting temperatures for M_xP_2 series were more prominently decreased by 10−11 °C with increasing acyl chain length. Following conjugation of the MA derivatives, the linear PEG chains are converted into multibranched domains, which appear to inhibit the tight packing of each individual PEG chain.

Table 1. Hydrophilic−Lipophilic Balance (HLB) and Critical Micelle Concentration (cmc) of AScM Series

	HLB[a]	cmc (M)		HLB[a]	cmc (M)
M_6P_2	15.4	4.45×10^{-5}	M_6P_5	17.8	8.64×10^{-5}
M_8P_2	14.7	4.76×10^{-6}	M_8P_5	17.5	7.87×10^{-6}
$M_{10}P_2$	14.1	2.60×10^{-6}	$M_{10}P_5$	17.2	1.20×10^{-6}
$M_{12}P_2$	13.6	1.27×10^{-6}	$M_{12}P_5$	16.8	1.25×10^{-7}

[a] The calculation was based on Griffin's theory.[54]

For comparison, the melting temperatures of the MA(x) series were measured. Similar to the M_xP_y series, increased chain length decreased the T_m: MA(6) > MA(8) > MA(10) > MA(12) corresponds to 170, 165, 159, and 156 °C, respectively. As the acyl branch length increases, the molecules (MA(x) or M_xP_y) are more separated and the free volume increases. As a result, the crystalline structure is more disrupted and the melting point is lowered.[42] The branch length effect is more dominant for MA(x) than its corresponding polymer M_xP_y, which has an additional long linear PEG component.

Critical Micelle Concentration. The cmc measurements of M_xP_y polymers were performed by fluorescence spectroscopy using pyrene as the probe[37−39] because pyrene preferentially partitions into the hydrophobic core of micelles from water. Upon changing the polarity of its microenvironment, pyrene undergoes a red shift (from 332 to 334.5 nm) in the excitation spectrum (Figure 1a). Fluorescence peak intensity ratios ($I_{334.5nm}/I_{332nm}$) were plotted against the logarithm of M_xP_y polymer concentrations to determine cmc, as the onset of micellization[38,39] (Figure 1b). Besides the red shift of the excitation band, the peak intensities decrease (Figure 1a) as the polymer concentrations increase. At high concentrations, pyrene partitions into the nonpolar micelle core, which lowers pyrene excitation energy. Upon dilution, the micellar structure becomes looser and eventually dissociates below the cmc, when pyrene is released from the dissociated micelle core. Throughout dilution, the excitation energy begins to increase as the polarity of the microenvironment changes.

The cmc values are most commonly employed to evaluate the thermodynamic stability of the polymeric micelles in aqueous solutions.[12] Compared to traditional surfactants (such as SDS, cmc = 8.6×10^{-3} M), amphiphilic polymers generally have remarkably lowered cmc values (usually at $\sim 10^{-6}$ M).[43] With such low cmc values, amphiphilic polymers can form highly stable micellar aggregates with low rates of dissociation in vivo.[44] Furthermore, amphiphilic polymers can stabilize the hydrophobic drugs inside the micelle core to achieve the sustained release and higher accumulation at specific physiological sites.[45] As shown in Table 1, the range of cmc values for the M_xP_y polymers is between 10^{-5} and 10^{-7} mol/L. The low cmc values illustrate the effectiveness of multibranched structure for stabilizing micellar aggregates. Other amphiphilic polymers with branched core-forming architectures, such as dendritic molecules[26] and pendant alkyl chains,[43] also show low cmc values around 10^{-6} M levels.

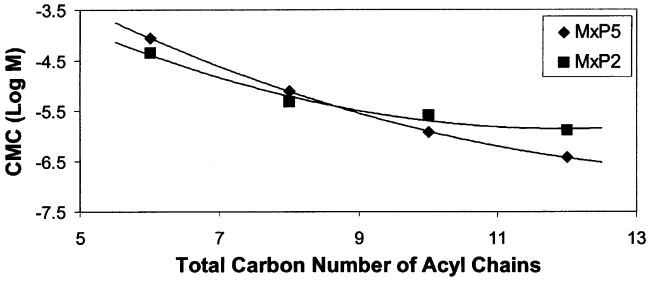

Figure 4. Relationship between acyl chain length and log cmc of the polymer series, M_xP_2 and M_xP_5.

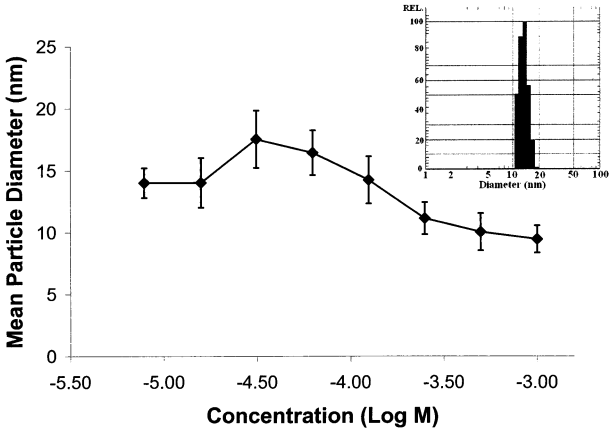

Figure 5. Diameter of micelles observed as a function of polymer ($M_{12}P_5$) concentration in aqueous solution measured by dynamic light scattering (DLS) methods. A representative DLS histogram is shown in the inset.

The core-forming blocks of M_xP_y polymers have chemically well-defined structures, and their main components are the four acyl chains. The nature or chemical composition of these core-forming block appears to be the dominate factor for the cmc values. Upon increasing the length of acyl chain, the cmc values are dramatically decreased (Figure 4). For example, in the M_xP_5 series, the cmc is lowered over 200 times (from 8.64×10^{-5} to 3.72×10^{-7} mol/L) as the total carbon number of each acyl chain increased from 6 to 12. The extent of branching is another key influence on cmc values. Besides the tetrabranched mucic acid derivatives, we also prepared dibranched tartaric acid derivatives with varying acyl chain lengths (data not shown), in which the corresponding polymer system has higher cmc values (10^{-4}–10^{-5} mol/L). Whereas the alkyl chains influence the cmc values, these values appear to be independent of the PEG chain length of the hydrophilic shell-forming block: the M_xP_2 and M_xP_5 series nearly overlap as illustrated in Figure 4.

Aggregation Size. Similar to conventional amphiphilic diblock copolymers,[30−32] M_xP_y self-assembles into micelles in an aqueous environment. Using dynamic light scattering, the aggregation sizes of the micelles were determined. All micellar aggregates have unimodal size distribution at around 10−20 nm within ±2 nm derivations. The sizes were independent of both PEG and alkyl chain lengths. Above the critical micelle concentrations, the aggregations are quite stable upon dilution. (Figure 5, $M_{12}P_5$ as an example) These stable, narrow-distributed nanometer micelles are expected to show extravasation efficacy for solid tumor tissues[46,47] and evade reticuloendothelial system uptake.[48−50]

Conclusions

A series of amphiphilic scorpion-like macromolecules (AScM) were successfully synthesized based on mucic acid, acyl chlorides, and monohydroxylated poly(ethylene glycol). We demonstrated that the micellar behavior of these polymeric amphiphiles can be carefully controlled by manipulating the molecular architecture of core-forming hydrophobic components. The multibranched structure of the hydrophobic region enhances the ability of the macromolecules to self-assemble into highly stable micellar aggregates. The low critical micelle concentrations (as low as 10^{-7} mol/L) and small particle sizes (10 nm to 20 nm) of these AScMs are appropriate, if not ideal, for lipophilic drug delivery and transport.[10,19,20]

Acknowledgment. The authors acknowledge the National Science Foundation (BES-9983272) for support of this work. We also thank Jelena Djordjevic (Pharmacy, Rutgers), Dr. Stephan S. Isied (Chemistry, Rutgers), and Dr. George Strauss (Chemistry, Rutgers) for their assistance.

References and Notes

(1) Kwon, G.; Kataoka, K. *Adv. Drug Delivery Rev.* **1995**, *16*, 295−309.
(2) La, S.; Okano, T.; Kataoka, K. *J. Pharm. Sci.* **1996**, *85*, 85−90.
(3) Jeong, B.; Bae, Y.; Lee, D.; Kim, S. *Nature (London)* **1997**, *388*, 860−862.
(4) Cammas, S.; Suzuki, K.; Sone, C.; Sakurai, Y.; Kataoka, K.; Okano, T. *J. Controlled Release* **1997**, *48*, 157−164.
(5) Inoue, T.; Chen, G.; Nakamae, K.; Hoffman, A. *J. Controlled Release* **1998**, *51*, 221−229.
(6) Allen, C.; Yu, Y.; Maysinger, D.; Eisenberg, A. *Bioconjugate Chem.* **1998**, *9*, 564−572.
(7) Kim, S.; Shin, I.; Lee, Y.; Cho, C.; Sung, Y. *J. Controlled Release* **1998**, *51*, 13−22.
(8) Bae, Y.; Huh, K.; Kim, Y.; Park, K.-H. *J. Controlled Release* **2000**, *64*, 3−13.
(9) Riley, T.; Stolnik, S.; Heald, C.; Xiong, C.; Garnett, M.; Illum, L.; Davis, S. *Langmuir* **2001**, *17*, 3168−3174.
(10) Otsuka, H.; Nagasaki, Y.; Kataoka, K. *Curr. Opin. Colloid Interface Sci.* **2001**, *6*, 3−10.
(11) Liu, L.; Li, C.; Li, X.; Yuan, Z.; An, Y.; He, B. *J. Appl. Polym. Sci.* **2001**, *80*, 1976−1982.
(12) Kataoka, K.; Harada, A.; Nagasaki, Y. *Adv. Drug Delivery Rev.* **2001**, *47*, 113−131.
(13) Rösler, A.; Vandermeulen, G.; Klok, H.-A. *Adv. Drug Delivery Rev.* **2001**, *53*, 95−108.
(14) Yu, J.; Jeong, Y.; Shim, Y.; Lim, G. *J. Appl. Polym. Sci.* **2002**, *85*, 2625−2634.
(15) Liggins, R.; Burt, H. *Adv. Drug Delivery Rev.* **2002**, *54*, 191−202.
(16) Gillies, E.; Frechet, J. *J. Am. Chem. Soc.* **2002**, *124*, 14137−14146.
(17) Bijsterbosch, M.; Van Berkel, T. *Adv. Drug Delivery Rev.* **1990**, *5*, 231−251.
(18) Torchilin, V.; Trubetskoy, V. *Adv. Drug Delivery Rev.* **1995**, *16*, 141−155.
(19) Torchilin, V. *J. Controlled Release* **2001**, *73*, 137−172.
(20) Nishikawa, M.; Takakura, Y.; Hashida, M. *Adv. Drug Delivery Rev.* **1996**, *21*, 135−155.
(21) Takakura, Y.; Mahato, R.; Nishikawa, M.; Hashida, M. *Adv. Drug Delivery Rev.* **1996**, *19*, 377−399.
(22) Hodoshima, N.; Udagawa, C.; Ando, T.; Fukuyasu, H.; Watanabe, H.; Nakabayashi, S. *Int. J. Pharm.* **1997**, *146*, 81−92.
(23) Junping, W.; Takayama, K.; Nagai, T.; Maitani, Y. *Int. J. Pharm.* **2003**, *251*, 13−21.
(24) Moghimi, S. M. *Adv. Drug Delivery Rev.* **1995**, *17*, 1.
(25) Kreig, A.; Lefebvre, A.; Hahn, H.; Balsara, N.; Qi, S.; Chakraborty, A.; Xenidou, M.; Hadjichristidis, N. *J. Chem. Phys.* **2001**, *115*, 6243−6251.
(26) Gitsov, I.; Lambrych, K.; Remnant, V.; Pracitto, R. *J. Polym. Sci., Part A: Polym. Chem.* **2000**, *38*, 2711−2727.

(27) Sternfeld, L.; Saunders, F. *J. Am. Chem. Soc.* **1937**, *59*, 2653−2658.
(28) Fonseca, A. *Can. J. Microbiol.* **1992**, *38*, 1242−1251.
(29) Schmalenberg, K.; Frauchiger, L.; Nikkhouy-Albers, L.; Uhrich, K. *Biomacromolecules* **2001**, *2*, 851−855.
(30) Gao, Z.; Eisenberg, A. *Macromolecules* **1993**, *26*, 7353−7360.
(31) Tuzar, Z.; Kratochvil, P. *Surf. Colloid Sci.* **1993**, *15*, 1−83.
(32) Cammas, S.; Kataoka, K. *Macromol. Chem. Phys.* **1995**, *196*, 1899−1905.
(33) Israelachvili, J. *Proc. Natl. Acad. Sci. U.S.A.* **1997**, *94*, 8378−8379.
(34) Vergara, A.; Paduano, L.; Sartorio, R. *Macromolecules* **2002**, *35*, 1389−1398.
(35) Wills, P.; Georgalis, Y.; Dijk, J.; Winzor, D. *Biophys. Chem.* **1995**, *57*, 37−46.
(36) Moore, J.; Stupp, S. *Macromolecules* **1990**, *23*, 65−70.
(37) Kalyanasundaram, K.; Thomas, J. *J. Am. Chem. Soc.* **1977**, *99*, 2039−2044.
(38) Wilhelm, M.; Zhao, C.-L.; Wang, Y.; Xu, R.; Winnik, M.; Mura, J.-L.; Riess, G.; Croucher, M. *Macromolecules* **1991**, *24*, 1033−1040.
(39) Astafieva, I.; Zhong, X.; Eisenberg, A. *Macromolecules* **1993**, *26*, 7339−7352.
(40) Reggelin, M.; Brenig, V.; Zur, C. *Org. Lett.* **2000**, *2*, 531−533.
(41) Kim, B.; Hrkach, J.; Langer, R. *Biomaterials* **2000**, *21*, 259−265.
(42) Lovisi, H.; Tavares, M.; da Silva, N.; de Menezes, S.; de Santa Maria, L.; Coutinho, F. *Polymer* **2001**, *42*, 9791−9799.
(43) Lavasanifar, A.; Samuel, J.; Kwon, G. *Colloids Surf., B: Biointerfaces* **2001**, *22*, 115−126.
(44) Allen, C.; Maysinger, D.; Eisenberg, A. *Colloids Surf., B: Biointerfaces* **1999**, *16*, 3−27.
(45) Kataoka, K.; Kwon, K.; Yokoyama, M.; Okano, T.; Sakurai, Y. *J. Controlled Release* **1993**, *24*, 119−132.
(46) Hobbs, S.; Monsky, W.; Yuan, F.; Roberts, W.; Griffith, L.; Torchilin, V.; Jain, R. *Proc. Natl. Acad. Sci. U.S.A.* **1998**, *95*, 4607−4612.
(47) Moghimi, S.; Hunter, A.; Murray, J. *Pharm. Rev.* **2001**, *53*, 283−318.
(48) Papisov, M. *Adv. Drug Delivery Rev.* **1995**, *16*, 127−139.
(49) Yokoyama, M.; Satoh, A.; Sakurai, Y.; Okano, T.; Matsumura, Y.; Kakizoe, T.; Kataoka, K. *J. Controlled Release* **1998**, *55*, 219−229.
(50) Nishiyama, N.; Kataoka, K. *J. Controlled Release* **2001**, *74*, 83−94.
(51) Chnari, E.; Tian, L.; Uhrich, K.; Moghe, P. Presented at the BMES National Meeting, Houston, TX, 2002.
(52) Greenwald, R.; Pendri, A.; Bolikal, D. *J. Org. Chem.* **1995**, *60*, 331−336.
(53) Sudimack, J.; Lee, R. *Adv. Drug Delivery Rev.* **2000**, *41*, 129−162.
(54) Griffin, W. *J. Soc. Cosmet. Chem* **1954**, *5*, 249−256.

MA030411A